Modeling the Oxidative Degradation of Ultra-High-Molecular-Weight Polyethylene

Vinay Medhekar,[1] Robert W. Thompson,[1] Aiguo Wang,[2] W. Grant McGimpsey[3]

[1]*Department of Chemical Engineering, Worcester Polytechnic Institute, 100 Institute Road, Worcester, Massachusetts 01609*
[2]*Stryker Howmedica Osteonics, 300 Commerce Street, Mahwah, New Jersey 07430*
[3]*Department of Chemistry and Biochemistry, Worcester Polytechnic Institute, 100 Institute Road, Worcester, Massachusetts 01609*

Received 25 February 2002; accepted 26 April 2002

ABSTRACT: Understanding the sequence of reactions that occur in ultra-high-molecular-weight polyethylene (UHMWPE) following ^{60}Co γ irradiation has been the focus of numerous experimental studies. In the study reported here, we have incorporated recent experimental findings into a mathematical model for UHMWPE oxidation. Simulation results for shelf aging and accelerated aging are presented. It is shown that very reasonable simulations of shelf-aging and accelerated-aging data can be obtained. It is also shown that simulations of shelf aging in reduced oxygen environments predict that the subsurface peaks of ketones will be shifted to the exterior surface. In vivo aging can be simulated if we assume that the oxygen level in the synovial fluid is about one-eighth that of atmospheric levels. Some reduced irradiation doses are predicted to significantly reduce the ketone formation for shelf-aging periods of up to 10 years. © 2002 Wiley Periodicals, Inc. J Appl Polym Sci 87: 814–826, 2003

Key words: polyethylene (PE); degradation; ageing

INTRODUCTION

Ultra-high-molecular-weight polyethylene (UHMWPE), with molecular weights of 3–6 $\times$ 10^6 g/mol, is widely used as a bearing surface in joint-replacement prostheses. It is estimated that in the United States 240,000 total hip prostheses and 245,000 total knee prostheses are implanted annually.[1] Prosthesis components must be sterilized before implantation. Ethylene oxide (ETO) was used in the 1960s and early 1970s but was replaced by γ sterilization with a ^{60}Co source. There were issues with worker exposure to ETO, ETO residuals, and the environmental release of ETO gas. γ sterilization to a nominal dose of 2.5 Mrad provided the certainty of sterilization without environmental and other concerns. γ sterilization was carried out on products sealed in a conventional, double-blister package filled with air. The clinical performance of total hip prostheses and total knee prostheses, γ-sterilized in air, has been excellent. The Swedish National Hip Arthroplasty Register[2] reports a revision rate of less than 1% for up to 10 years of implantation with an 80% survivorship at 20 years. Long-term follow-up of total knee replacements, γ-sterilized in air, also demonstrates a revision rate of about 1% per year.[3]

In the 1980s and early 1990s, there was a growing concern over osteolysis around total hip replacements.[4–8] This led to new investigations into the structure–property relationships with UHMWPE. One area of study was the effect of γ irradiation, in conjunction with exposure to oxygen, on the structural changes to UHMWPE. By the mid 1990s, these studies had been extended to include total-knee-replacement prostheses.

The γ sterilization of UHMWPE results in the formation of free radicals, which can crosslink neighboring molecules, increasing the molecular weight of the polymer. Alternatively, free radicals can react with oxygen, ultimately resulting in chain scission and a reduction in molecular weight. The oxidation process can continue for many years if there is oxygen available. However, this process causes C—H and C—C bond scission, which then initiates the oxidation of the free radicals formed, followed by a series of reactions leading to the potential formation of hydroperoxides, alcohols, carbonyls, acids, and esters.[9–14] If components are stored in air for a considerable time, a maximum oxidation at a depth of 1–2 mm in the subsurface can develop, with a consequent loss of mechanical properties due to molecular weight reduction.[12–15] It has been documented that this process leads to smaller polymer chains and a loss of mechanical strength and abrasion resistance.[14,16–18] Therefore, be-

Correspondence to: R. W. Thompson (rwt@wpi.edu).
Contract grant sponsors: Stryker Howmedica Osteonics; Chemical Engineering Department, Worcester Polytechnic Institute.

ginning in the mid 1990s, companies changed the sterilization process either by avoiding the use of ionizing radiation or by excluding air from the packaging while retaining γ sterilization. The retention of γ sterilization was based on the realization, in the mid 1990s, that crosslinking at the nominal 2.5 Mrad dose reduced wear by some 50% with respect to products sterilized by nonionizing techniques.

Although the process of γ sterilization in air is no longer employed, there is still interest in understanding the chemical changes that occur. These changes are complex, and there are many different pathways possible for the reactions. There have been several models proposed for oxidation changes, and there is disagreement over the relative importance of the different reactions. Recently, there has been an attempt to model the spatial and temporal changes that take place with oxidation.[12] The model is not consistent with recent experimental data, as will be discussed later. However, the approach is valuable in that the validation of a model explaining the chemical changes subsequent to γ sterilization in air allows an extension to the study of other situations. For example, a validated model could be used to study the effect of different packaging atmospheres, the use of accelerated-aging methods,[13,14,19–21] and the progress of in vivo oxidation. The purpose of this article is to report on the development of a model to allow such tasks. The model is based on an extensive examination of the proposed chemical pathways in the literature and on published data on measured levels of chemical species as a function of time and position in UHMWPE after γ sterilization in air. The experimental data for the simulation were obtained from the literature[12,21] and from our laboratories.[13,14]

MODELS

Recently, Daly and Yin[12] published the results of a model developed to simulate the spatial and temporal variation of carbonyls in shelf-aged UHMWPE samples. They made several assumptions in developing their model, some of which were of little consequence (e.g., the sample was oxygen-free when irradiated), whereas others will be shown to have more impact on the simulations of recently reported data. For example, Coote et al.[13] recently showed, with an NO derivatization technique, that alcohols were not observed in his irradiated samples. Additionally, the same technique revealed that hydroperoxides were present in his shelf-aged and accelerated-aged samples. Those experimental results appeared after Daly and Yin's work was published, so they could not be expected to be aware of those results. However, they added a free radical, R $\cdot$, to both sides of a chemical reaction [their reaction (12)] without explanation and then included an [R $\cdot$] term in their rate equations; this step was difficult to understand in the context of their listed chemical reactions.

Coote et al.[13] recently summarized the oxidation reactions reported in the literature following the irradiation of UHMWPE. Recent studies[13,21] have provided information about the shelf aging and accelerated aging of UHMWPE, which should be simulated by a model appropriate for this process:

1. Alcohols were not observed to form in either shelf-aged or accelerated-aged samples.[13] Flynn[14] made similar observations.
2. Hydroperoxides were noted to form within 2 years of shelf aging and to remain at that constant level for up to 8 years of shelf aging. During accelerated aging, the hydroperoxide concentration increased within the first 3 mm from the surface for 5 weeks, and then the concentration decreased in that region.[13]
3. Carbonyls were observed to remain at a low level at the sample surface for up to 8 years of shelf aging, whereas a subsurface peak at about 2 mm below the surface continued to evolve. In accelerated aging, the carbonyl concentration at the surface continued to increase for up to 13 weeks.[13] Flynn[14] made similar observations.
4. The subsurface peak approached the surface with an increased irradiation dose. The concentration of carbonyls formed at the surface increased with increases in the irradiation dose.[21]

As a result of the absence of alcohols, we have ignored the alcohol formation reactions in the four models described. We have dealt with the hydroperoxide formation and decomposition steps differently than Daly and Yin.[12]

Model I: reversible formation of ROOH

The reactions proposed for model I were based on the presumption that the accelerated-aging data reported by Coote et al.[13] suggested the reversible formation of hydroperoxides:

$$R\cdot + O_2 \rightarrow RO_2\cdot \qquad \text{(I-1)}$$

$$RO_2\cdot + RH \leftrightarrow ROOH + R\cdot \qquad \text{(I-2)}$$

$$RO_2\cdot + R\cdot \rightarrow 2RCO + 2R\cdot \qquad \text{(I-3)}$$

Reaction (I-3) is actually the result of the rapid decomposition of ROOR species to form RO $\cdot$ species, which in turn react rapidly to give a carbonyl compound, RCO, and another free radical, R $\cdot$, along the polymer

backbone. However, the net reaction (I-3) has been reported previously in the literature.[22]

Model II: irreversible formation of ROOH

Another reaction pathway explaining the hydroperoxide results reported by Coote et al.[13] is that hydroperoxides decompose into acids, esters, and other oxygenated byproducts. It has been reported previously that hydroperoxides can decompose into acids, esters (with alcohols), and aldehydes;[11,23,24] however the formation of ketones from hydroperoxides by the cage reaction has been shown in the literature as unlikely to occur,[25] so we neglected that reaction in our simulation. The resulting chemical reactions for model II are

$$R\cdot + O_2 \rightarrow RO_2\cdot \quad \text{(II-1)}$$

$$RO_2\cdot + RH \rightarrow ROOH + R\cdot \quad \text{(II-2)}$$

$$RO_2\cdot + R\cdot \rightarrow 2RCO + 2R\cdot \quad \text{(II-3)}$$

$$ROOH \rightarrow \text{acids, esters, aldehydes} \quad \text{(II-4)}$$

Unfortunately, Coote et al. did not systematically monitor the evolution of acids or esters, so their formation in their samples was not demonstrated.

Model III: hydroperoxide-catalyzed ketone formation

Petrůj and Marchal[25] noted that hydroperoxides can participate in the formation of ketones but can be preserved in the process by transfer to another point on the polymer chain. In our notation, their hydroperoxide-catalyzed ketone formation reaction is written as follows:

$$RO_2\cdot + ROOH \rightarrow ROOH + RCO + HO\cdot \quad \text{(III-1a)}$$

$$HO\cdot + RH \rightarrow R\cdot + H_2O \quad \text{(III-2a)}$$

Reaction (III-1a) is actually two steps combined to produce a ketone and a hydroxyl radical. If the hydroxy radical is assumed to be short-lived, the two reaction steps shown can be combined to yield one, as shown in reaction (III-4). Even though Coote et al.[13] did not report detecting water in their UHMWPE samples, water would be expected to vaporize quickly once the block sample was microtomed to produce films approximately 50 μm thick for depth profiling. Consequently, the reaction steps in model III are

$$R\cdot + O_2 \rightarrow RO_2\cdot \quad \text{(III-1)}$$

$$RO_2\cdot + RH \rightarrow ROOH + R\cdot \quad \text{(III-2)}$$

$$RO_2\cdot + R\cdot \rightarrow 2RCO + 2R\cdot \quad \text{(III-3)}$$

$$RO_2\cdot + ROOH + RH \rightarrow RCO + ROOH + R\cdot + H_2O \quad \text{(III-4)}$$

$$ROOH \rightarrow \text{acids, esters, aldehydes} \quad \text{(III-5)}$$

Model IV: second-generation free-radical formation

It has been proposed that the free radicals formed during γ-irradiation sterilization possess a higher energy than the free radicals created as part of the chain reactions after the irradiation.[26] Specifically, the free radicals formed by the transformation of $RO_2\cdot$ into ROOH may react with oxygen to form $RO_2\cdot$ again, but that new $RO_2\cdot$ radical is not sufficiently excited to form hydroperoxides again. According to this concept, model IV is written as follows:

$$R\cdot + O_2 \rightarrow RO_2\cdot \quad \text{(IV-1)}$$

$$RO_2\cdot + RH \rightarrow ROOH + R'\cdot \quad \text{(IV-2)}$$

$$R'\cdot + O_2 \rightarrow R'O_2\cdot \quad \text{(IV-3)}$$

$$R'\cdot + R'O_2\cdot \rightarrow 2R'CO + 2R'\cdot \quad \text{(IV-4)}$$

$$R'O_2\cdot + ROOH + RH \rightarrow RCO + ROOH + R'\cdot + H_2O \quad \text{(IV-5)}$$

$$ROOH \rightarrow \text{acids, esters, aldehydes} \quad \text{(IV-6)}$$

In these expressions, the radicals formed by irradiation are designated $R\cdot$, whereas the second-generation, less energetic radicals are designated by $R'\cdot$. We further assumed that the initial and second-generation free-radical species could participate in reactions (IV-4) and (IV-5) with equal probability. We also retained the reaction step suggested by Petrůj and Marchal[25] in model IV, that is, reaction (IV-5).

SIMULATION RESULTS

Preliminaries

The oxidative degradation process was assumed to begin at the moment that free-radical formation by ^{60}Co irradiation was completed. The time of irradiation was negligible (i.e., minutes) compared with the timescale of oxidation simulation (i.e., weeks to years), and so oxidation occurring during the irradiation period was neglected for simplicity. Partial differential equations describing the simultaneous diffusion of oxygen and the formation and consumption reactions noted in each model were developed. In doing so, we

TABLE I
Values of the System Parameters[12]

Parameter	Value	Units
Length of the polymer sample, L	1.42	cm
R* (initial alkyl radical concentration)	7.60×10^{-4}	g mol/L
D_{O2} (diffusivity of oxygen in PE)	6.40×10^{-10}	dm^2/s
Age of the component	10.9	years

assumed that each reaction rate term was first-order in each component of the reaction. The concentrations of oxygen, free radicals, and each of the oxygenated products were computed as functions of position, in a single Cartesian dimension into the sample, and time. The origin, $x = 0$, was set at the sample surface.

Oxygen was assumed to be present initially at the equilibrium solubility throughout the sample and to diffuse into the polymer as oxygen was consumed by the reaction. The surface concentration of oxygen, that is, the boundary condition, was taken to be the equilibrium solubility concentration. Solubility and diffusion coefficient parameters were taken from Daly and Yin[12] or Pauly.[27]

A crystallinity of 50% was assumed for UHMWPE.[28] We assumed that the free radicals generated were uniformly distributed between the two domains,[13,21] that the crystalline domains were essentially impermeable to oxygen,[21] and that the free radicals in the crystalline domains remained inside those domains. We also assumed that 80% of the free radicals initially formed in the amorphous region crosslinked rather quickly, leaving 20% (i.e., 10% of the total formed) to participate in the oxidation reactions.[9,29–31] Furthermore, it was assumed that the free radicals trapped in the crystalline regions were released to participate in the degradation reactions only at elevated temperatures.[32]

The systems of partial differential equations were solved with a forward difference explicit method employing a Compaq® 500 MHz Alpha Professional Workstation XP1000. The program was written in Fortran 77. Simulation results were compared with the ketone data reported by Daly and Yin[12] at 10.9 years, and adjustments were made in the rate parameters with a Levenberg–Marquardt method for the optimization of nonlinear systems. Adjustments were made in the values of the rate constants until the best fit of the simulation to the data was found. This procedure was tested with the Daly and Yin model[12] to determine the best rate constants to fit their ketone data at 10.9 years. The values that we obtained for their rate constants, k_1 and k_2, were within 3% of theirs and gave essentially the same fit to their data as they reported. Once rate parameters were found for our various models, the simulations of species concentrations at intermediate times were carried out to verify that hydroperoxide and ketone profiles conformed to their data and that of Coote et al.[13] The simulations also gave results like those reported by Yeom et al.,[21] as will be shown later.

First observations

Table I contains the values of the system parameters that formed the base case for the simulations. The fit of the simulated ketone profiles with the data from Daly and Yin[12] was generally good with all four models but was not sufficient to discriminate between the models. However, the first three models were incapable of describing the hydroperoxide profiles generated by Coote et al.[13] for the shelf-aged and accelerated-aged samples. Therefore, the remainder of this report focuses only on the simulations with model IV.

Simulation results from model IV

Shelf-aging results

The partial differential equations comprising model IV are shown in the Appendix. The rate constants found with the Levenberg–Marquardt algorithm to minimize the error between simulated results and experimental data are listed in Table II. The simulation results and the experimental data for ketones versus the dimensionless position in the sample are shown in Figure 1. The external surface of the sample is at the axial position $x/L = 0$, whereas $x/L = 0.5$ is at the center of the sample (where x = depth into the polymer sample from the surface and L = length of polymer sample as given in Table 1). The fit of the ketone data at 10.9 years of room-temperature shelf aging[12] by the simulations and the evolution of the predicted profiles over time, were essentially the same with all four models. The predicted subsurface peak appears to move slightly deeper into the sample with increased shelf aging but certainly not to the extent that Daly and Yin's[12] data between 5.8 and 10.9 years show. Coote et al.[13] and Flynn[14] showed data that more closely resembled the predictions of the model, insofar as the

TABLE II
Rate Constants Obtained for the Best Fit for Model IV

Parameter	Value	Units
k_1	5.00×10^{-2}	L/mol s
k_2	3.60×10^{-4}	L/mol s
k_3	5.70×10^{-3}	L/mol s
k_4	3.90×10^{-4}	L/mol s
k_5	3.00×10^{-8}	L^2/mol^2 s
k_6	1.00×10^{-14}	1/s
R* (initial alkyl radical concentration)	7.60×10^{-4}	g mol/L
D_{O2} (diffusivity of oxygen in PE)	6.40×10^{-10}	dm^2/s

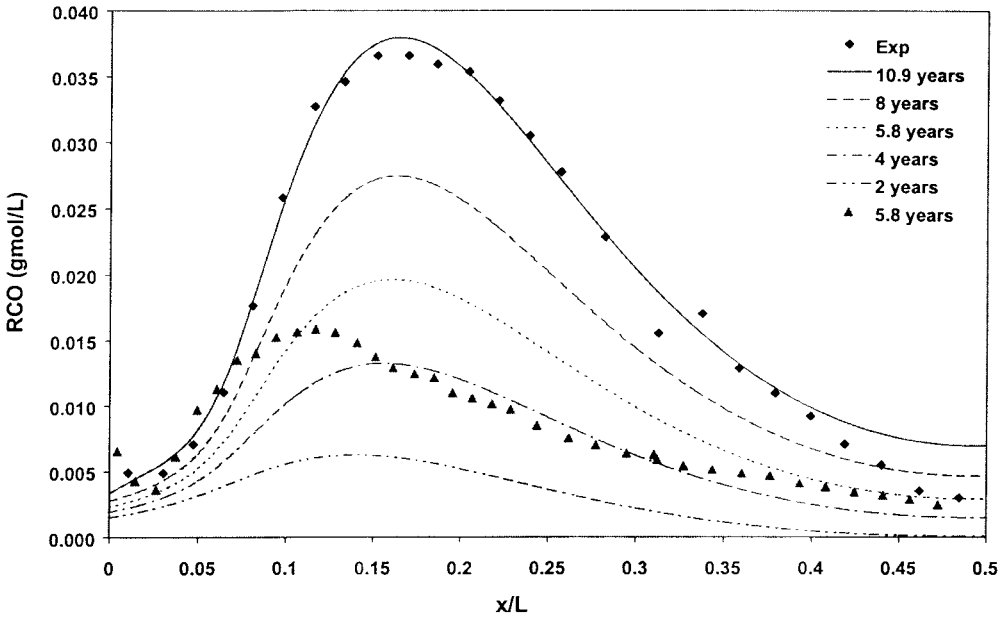

Figure 1 Simulated and experimental ketone concentration profiles during shelf aging. The data have been replotted from Daly and Yin.[12]

subsurface peak movement is concerned; that is, they reported less drift.

Figure 2 shows the predicted hydroperoxide profiles, that is, [ROOH] versus the position in the sample over the same aging time. Except for a small deviation deep into the sample in the 2-year sample, the prediction is that [ROOH] should remain at about a fixed level during the entire 8-year aging period. Although Coote et al.[13] showed that the hydroperoxides did not change over the 8-year aging period, they showed a relatively higher [ROOH] at the surface (their Fig. 4), which dropped within the first 250 μm below the surface. They noted, however, that making measurements precisely at the surface with their IR technique was prone to error there. Because our simulations do not show that feature in the [ROOH] profiles near the surface, it also is possible that within that narrow skin layer the polymer properties were different. The slight decrease in [ROOH] in the bulk of the sample was reproduced by these simulations.

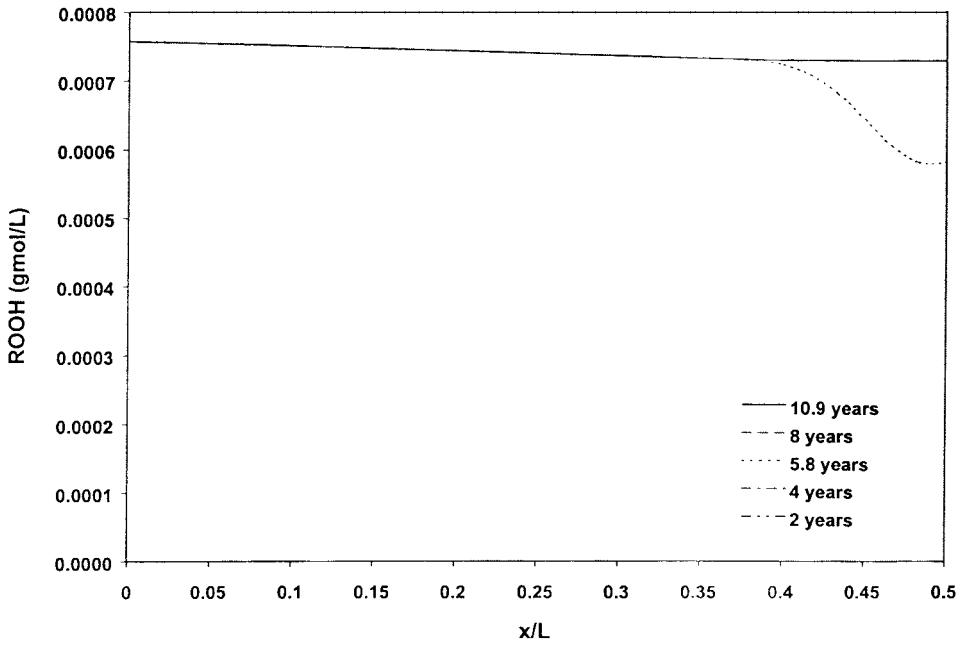

Figure 2 Simulated hydroperoxide concentration profiles during shelf aging.

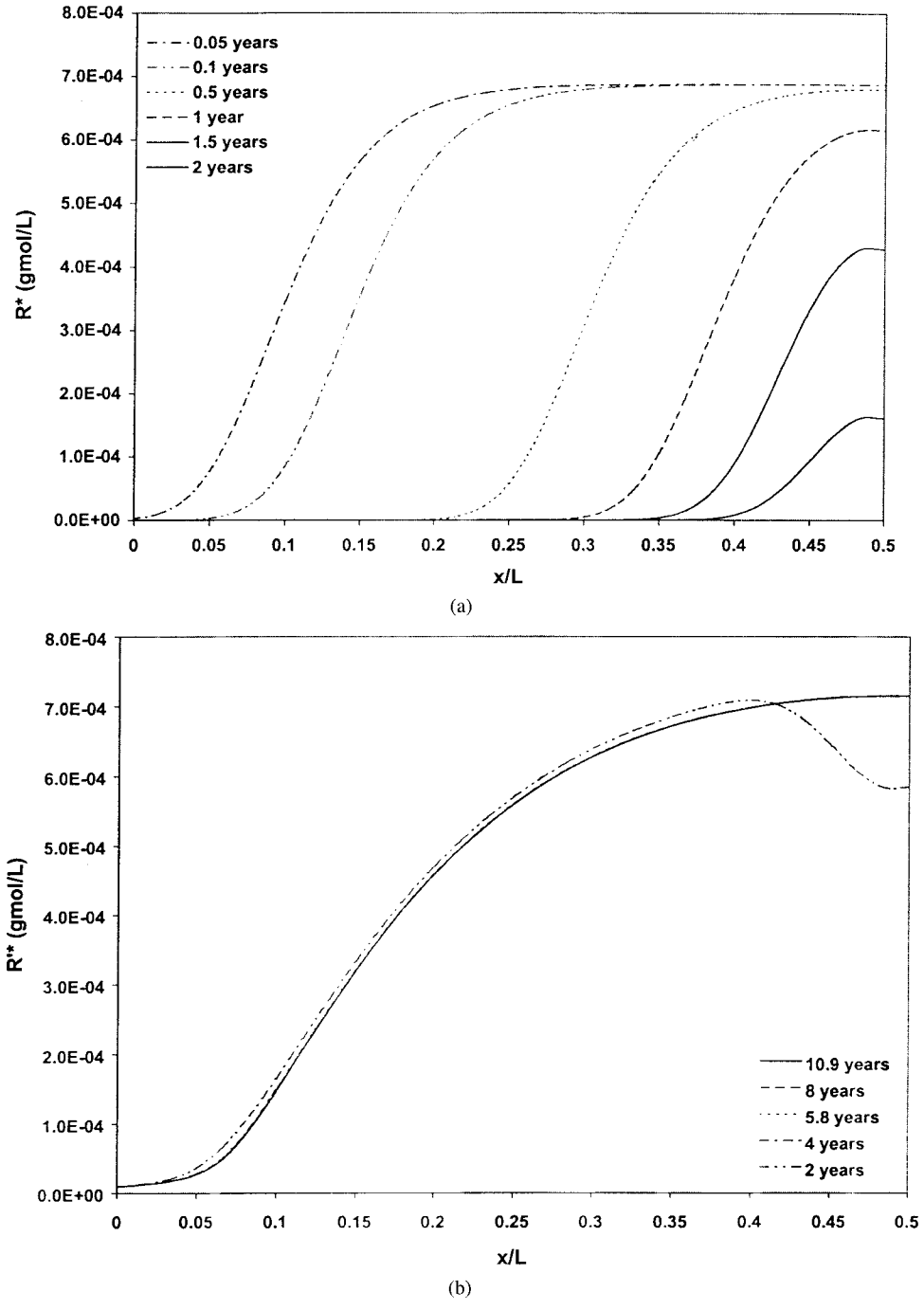

Figure 3 Simulated (a) first-generation and (b) second-generation alkyl free-radical concentration profiles during shelf aging. Note the different times used.

These results indicated that the hydroperoxides were formed by reaction (IV-2) and that they remained at essentially a constant concentration over time because the hydroperoxide decomposition rate was so low; that is, k_6 was very small. The reaction step reported by Petrůj and Marchal[25] was not very important in this analysis by virtue of the optimization algorithm also selecting a small value for rate constant k_5.

These results suggest that the key species in the degradation reactions are the free radicals and the peroxy radicals. Figure 3(a,b) shows the predicted concentration profiles of the two free-radical species. Figure 4(a,b) shows the corresponding predicted concentration profiles of the two peroxy radical species. As expected by the nature of model IV, the primary species, R · and RO_2 · , eventually disappear, whereas the less energetic species, R′ · and R′O_2 · , reach a

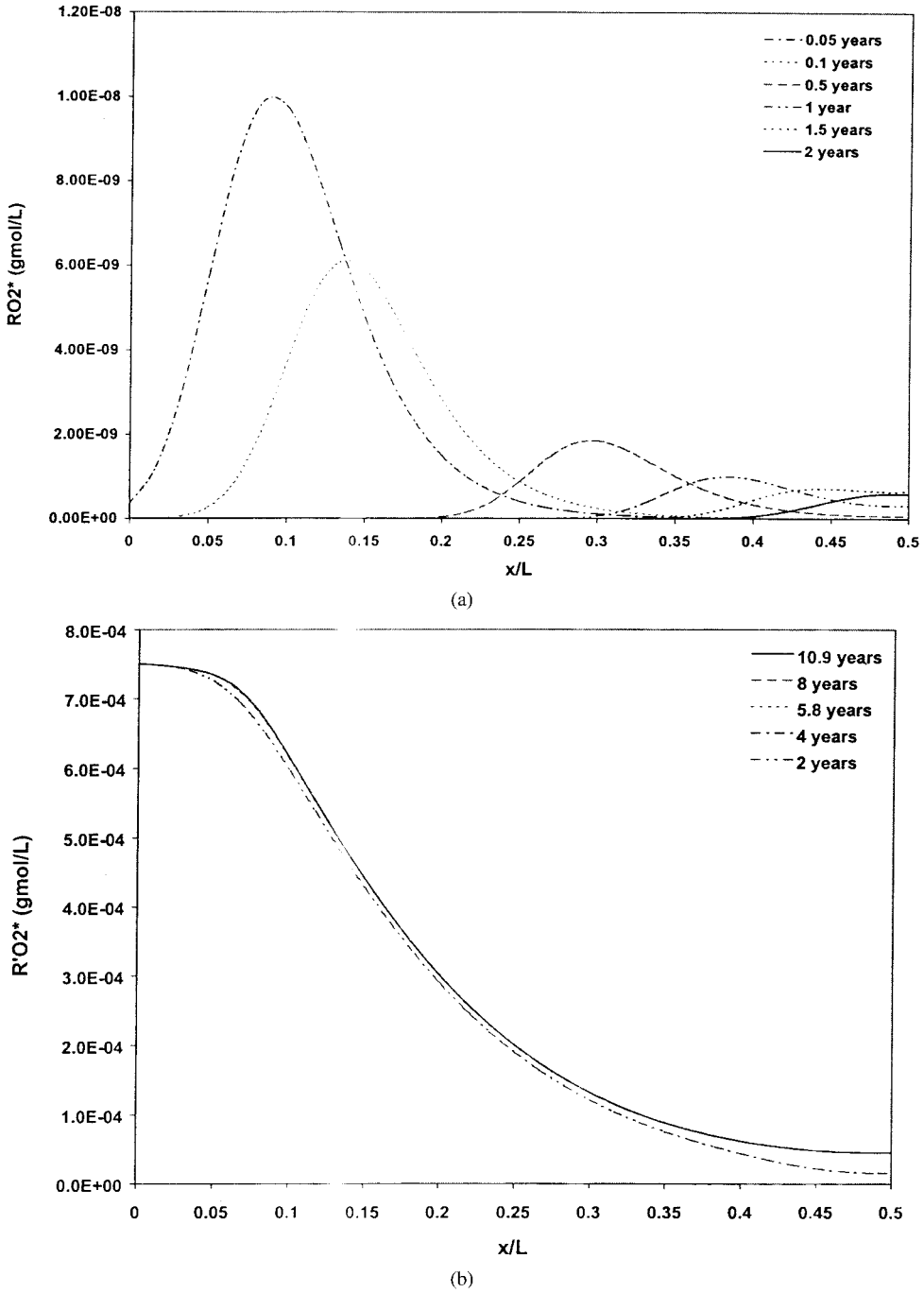

Figure 4 Simulated (a) first-generation and (b) second-generation peroxy free-radical concentration profiles during shelf aging. Note the different times used.

quasi-steady-state profile in the sample rather early on in the shelf-aging period. These second-generation radicals sustain the chain reactions leading to ketone formation.

Figure 5 shows the predicted dissolved oxygen profile in the bulk of the sample during the shelf-aging period, and it has been assumed that the sample was saturated with oxygen at its equilibrium solubility level at $t = 0$. These simulations show that the oxygen profile is established rather quickly in the aging period and that Daly and Yin's[12] assumption of $[O_2] = 0$ at $t = 0$ did not have a significant effect on their simulation results.

Shelf aging in reduced oxygen environments

Figure 6 shows the predicted results of shelf aging in reduced oxygen atmospheres, which might be characteristic of oxygen-lean inert package environments such as those evaluated by Coote et al.[13] The simula-

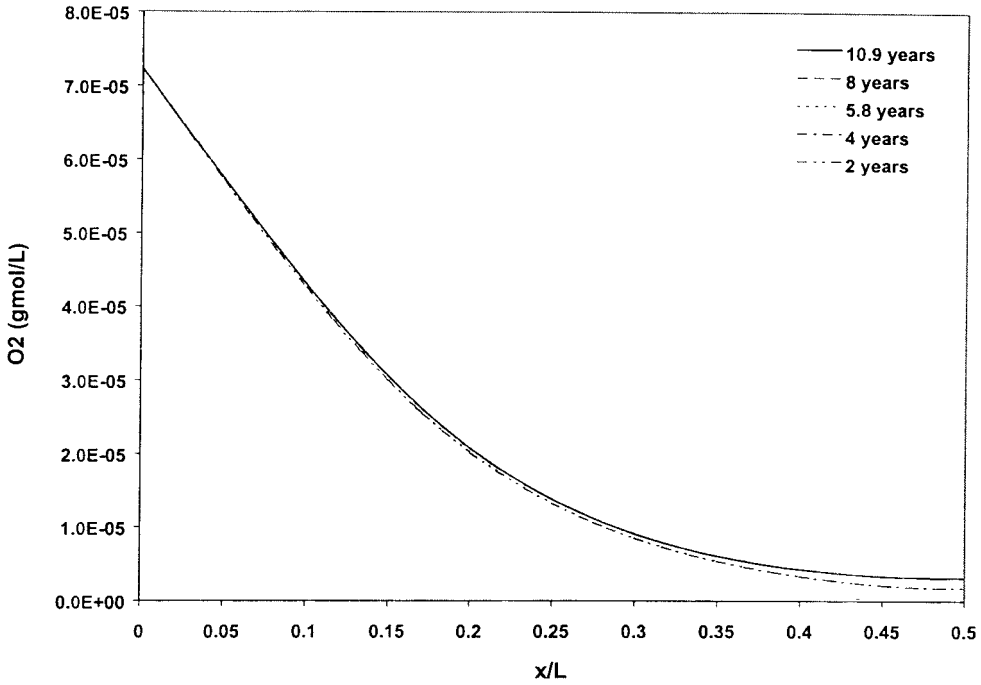

Figure 5 Simulated dissolved oxygen in a UHMWPE sample during shelf aging.

tions of 10.9 years of aging in these atmospheres show that the subsurface peak shifts toward the surface of the sample and eventually disappears. That is, the predicted maximum ketone concentration exists at the surface for oxygen environments having about 6% oxygen or less.

One might also note that the curves representing 2–3% oxygen should be comparable to the dissolved oxygen levels in the human body (ca. one-eighth of the normal atmospheric oxygen partial pressure). As such, these profiles would represent the oxidation to be expected if an orthopedic component were implanted immediately after irradiation, that is, without any shelf aging. These predictions do not account for any shelf aging before implantation or for changes in the polymer properties when the polymer is surrounded by synovial fluid. In their Figures 8 and 9, Yeom et al.[21] showed oxidation

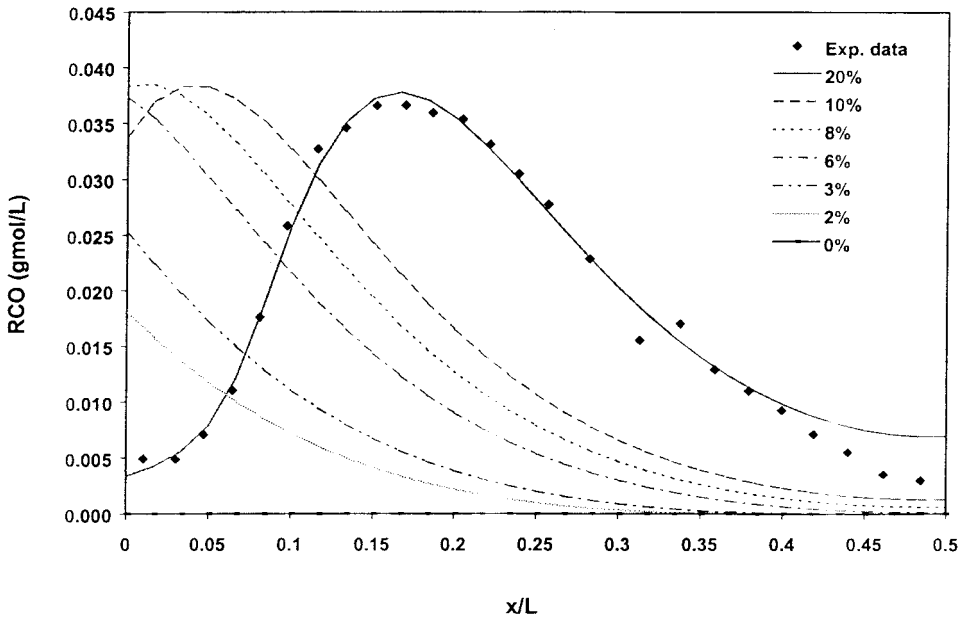

Figure 6 Predicted ketone formation after 10.9 years of shelf aging in reduced oxygen environments. The data are from Daly and Yin.[12]

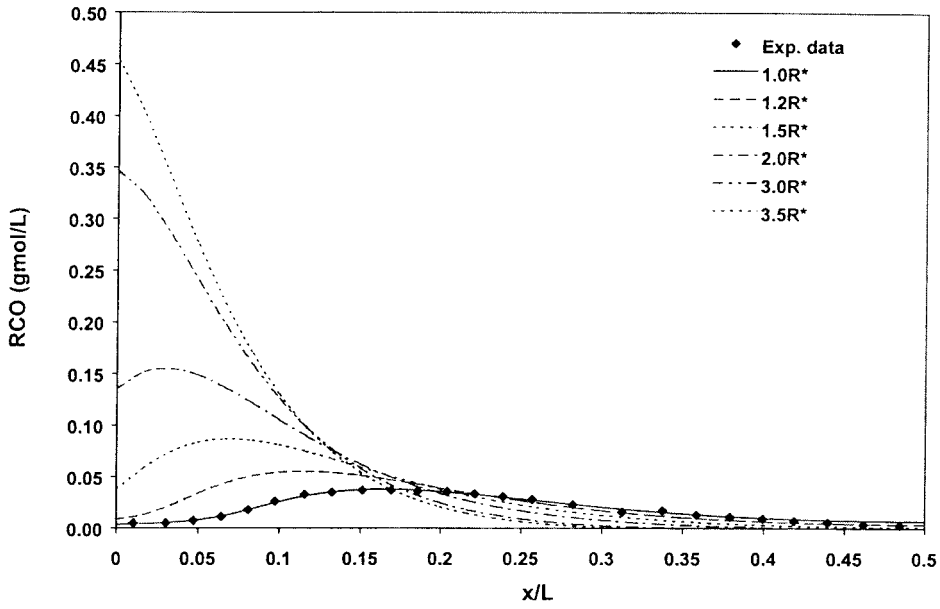

Figure 7 Predicted ketone concentration profiles after 10.9 years of shelf aging after irradiation with higher than normal doses. The data are from Daly and Yin.[12]

profiles for retrieved hip cups after 4 years in vivo. In a worn area, they showed profiles similar to our predictions in Figure 6, whereas in a nonworn area, a subsurface peak of carbonyls was observed roughly 0.5 mm below the surface. We note that a comparison with their data is not possible because they did not report carbonyl profiles in shelf-aged pieces after 4 years. We also lack information on the ex vivo age of the piece before implanting or possible physical changes in UHMWPE when in the body.

The model can be used to predict the oxidation profiles of implants if we presume that the oxidation due to shelf aging at the time of implantation is superimposed on subsequent oxidation in the body. In effect, the model could then be used to develop protocols for maximum shelf aging, which would protect the component from oxidative failure in the body.

Shelf aging after different radiation doses

The model can be used to investigate the effects of using different radiation doses to sterilize the components before shelf-aging storage. Figure 7 shows the effects of using higher radiation doses, simulated by an increase in the initial concentration of free radicals, subject to the same assumptions about their location and extent of rapid crosslinking. Yeom et al.[21] made similar observations and showed (in their Fig. 6) that higher radiation doses led to higher carbonyl formation with the subsurface peak moved toward the surface. Figure 8, however, shows the effects of using lower radiation doses, that is, with lower initial free-radical concentrations in the simulations. Using higher radiation levels is predicted to increase the absolute level of ketones formed in the shelf-aging period and to move the subsurface maximum toward the external surface. Using lower doses, by contrast, is predicted to cause the opposite trend; that is, the subsurface peak becomes smaller and moves deeper into the sample. These predictions are consistent with the data reported by Yeom et al.[21]

There appeared to be a marked difference between $0.80[R\cdot]_i$ and $0.60[R\cdot]_i$, which caused a significant decrease in the predicted ketone levels after 10.9 years of shelf aging. The cause for this dramatic drop is the significant decrease in the concentration of second-generation free radicals, as shown in Figure 9. That is, below a certain critical level of the initial free radicals formed, $[R_i\cdot]_i$, there are not enough second-generation free radicals, formed by reaction (IV-2), to sustain a significant level of ketone formation by the subsequent chain reactions.

These predictions could be quite beneficial in reducing oxidative degradation but have not yet been tested experimentally.

Accelerated-aging simulations

There is interest in developing accelerated-aging tests that can show the oxidative degradation behavior to be expected of new materials in shorter times. Unfortunately, however, elevated-temperature tests typically result in different ketone concentration profiles in UHMWPE samples that make direct comparisons difficult.[13,14] Ketone formation is typically quite a bit higher at elevated temperatures (ca. 80°C), reaction

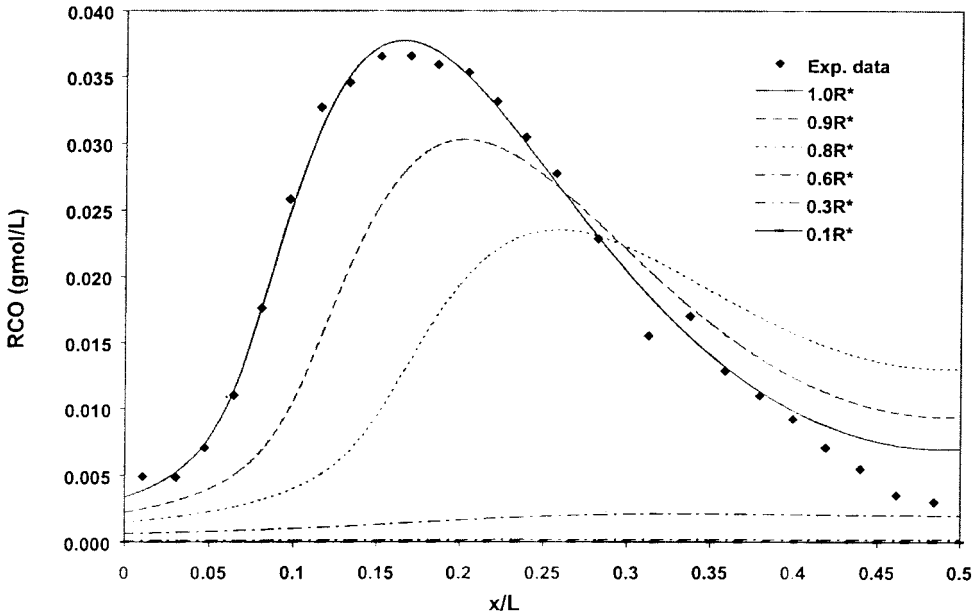

Figure 8 Predicted ketone concentration profiles after 10.9 years of shelf aging after irradiation with lower than normal irradiation doses. The data are from Daly and Yin.[12]

rates are much faster, and the subsurface peak typically is not manifested.

Higher temperatures result in higher reaction rate constants and higher diffusion coefficients. We arbitrarily increased most of the rate constants by a factor of 10. However, previous studies[23,33] have shown that hydroperoxides decompose to a far greater extent at elevated temperatures. That was taken into account by an increase in the hydroperoxide decomposition rate constant, k_6, by a larger factor to force that reaction to become more prominent. The diffusion coefficient was computed to increase by about a factor of 10 with a reported activation energy.[27] These values are summarized in Table III. We also assumed that the free radicals bound in the crystalline regions would be liberated and captured by available dissolved oxygen.[32]

Figure 10 shows the predicted ketone concentration profiles during accelerated aging with these modifications to the model IV framework. As expected, the

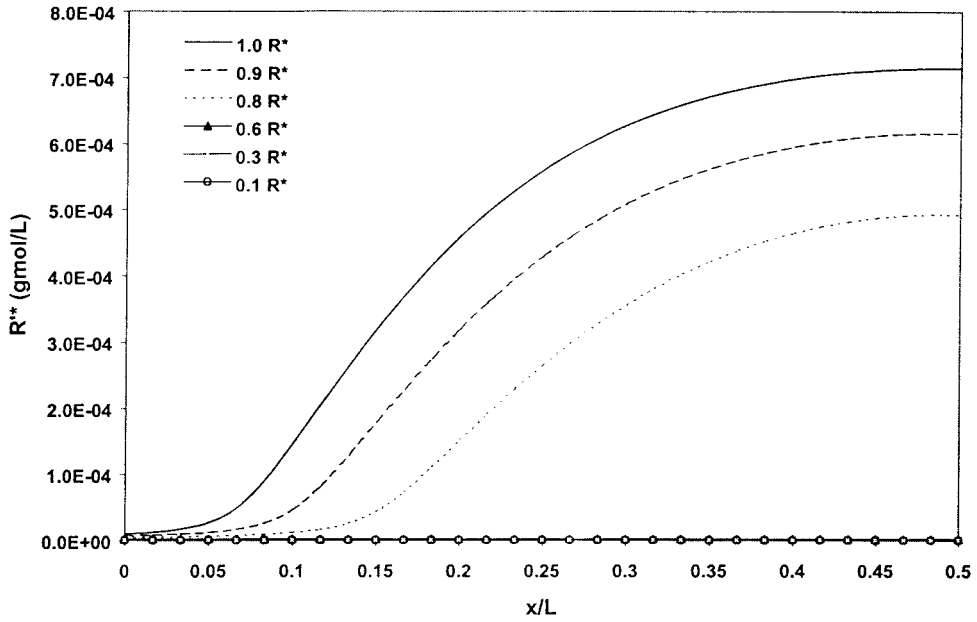

Figure 9 Predicted second-generation alkyl free-radical concentration profiles after 10.9 years of shelf aging with lower than normal irradiation doses.

TABLE III
Rate Constants for Accelerated Aging for Model IV

Parameter	Value	Units
k_1	5.00×10^{-1}	L/mol s
k_2	3.60×10^{-3}	L/mol s
k_3	5.50×10^{-2}	L/mol s
k_4	3.90×10^{-3}	L/mol s
k_5	3.00×10^{-7}	L^2/mol^2 s
k_6	5.00×10^{-7}	1/s
R* (initial alkyl radical concentration)	4.25×10^{-3}	g mol/L
D_{O2} (diffusivity of oxygen in PE)	6.40×10^{-9}	dm^2/s

ketones continued to form, and the subsurface peak observed in shelf-aging studies was changed to a maximum at the surface. These results are similar in their features to those shown with increased radiation doses, but the profiles emerge much more quickly. It must be realized that increasing the rate constants by a factor of 10 was arbitrary and was done just to illustrate the effect that higher temperatures might have; in fact, the rate constants might all increase to different extents.

The predicted hydroperoxide concentration profiles are shown in Figure 11. The essential feature of these predictions is that the hydroperoxide concentration is predicted to increase in a region near the surface and then begin to decrease in that region as the hydroperoxide decomposition products form by reaction (IV-6). The timescales of these predictions do not resemble Coote et al.'s data[13] precisely, but clearly the trends are correctly represented.

CONCLUSIONS

It is most important to state initially that a model is not necessarily proven to be an accurate representation of the real chemistry of a process just because it fits some experimental data. Certainly, the absolute numerical values of the rate parameters must be considered with skepticism. However, we can say that there are certain features of the models that appear to be consistent with experimental observations and with other reports in the literature. Other features of the simulations suggest certain new experimental studies that should be undertaken.

It would appear that reactions like those posed in eqs. (IV-1)–(IV-4) are the essential part of the shelf-aging model for oxidative degradation. The reaction suggested by Petrůj and Marchal,[25] reaction (IV-5), does not appear to be essential for the model simulations to reasonably portray experimental observations. Experiments could be devised that would determine whether or not that reaction is involved in the reaction sequence to corroborate this conclusion.

The decomposition of hydroperoxides, as per reaction (IV-6), appears to be necessary to explain the initial formation and then subsequent demise of hydroperoxides at elevated temperatures. It appears to be unimportant in shelf-aging oxidative degradation, and this conclusion implies that hydroperoxides are not a reaction pathway to oxidative degradation, that is, the formation of ketones, but are only a species in which a relatively small amount of oxygen has been captured.

Once the model was developed, it was a straightforward matter to modify parameters and system conditions to simulate the predicted behavior of reduced ox-

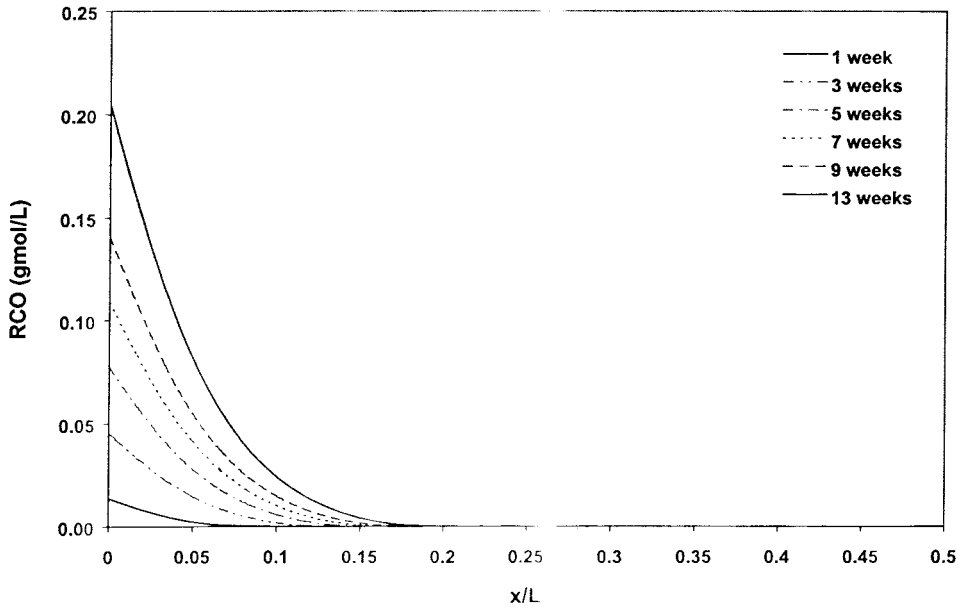

Figure 10 Simulated evolving ketone concentration profiles at accelerated-aging conditions, that is, simulated elevated temperatures.

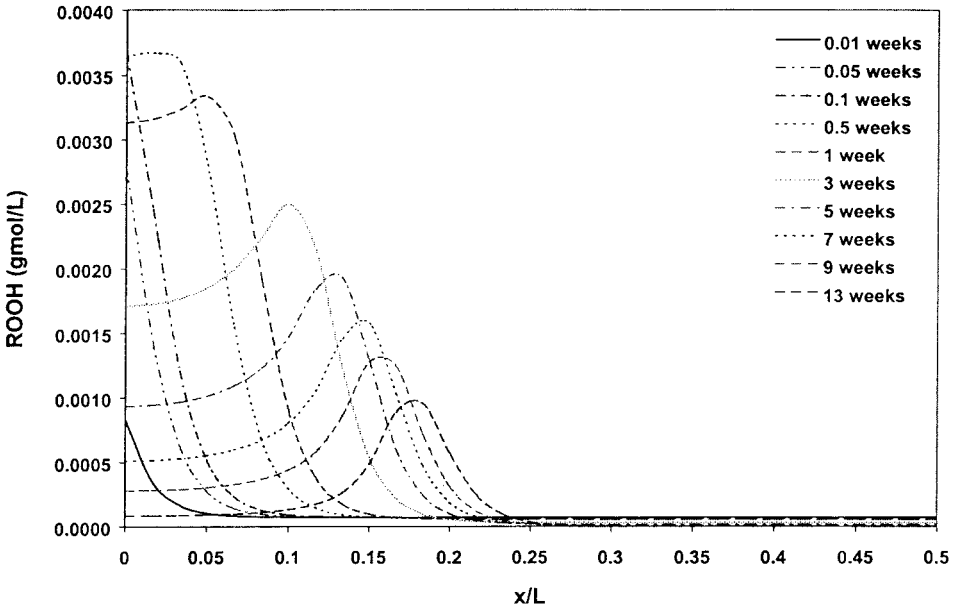

Figure 11 Simulated evolving hydroperoxide concentration profiles at accelerated-aging conditions, that is, simulated elevated temperatures.

ygen environments and the use of higher or lower radiation doses. One rather dramatic prediction was that using a radiation dose on the order of 60% of that reported by Daly and Yin[12] would result in significantly lower ketone formation. This result was due to the significant reduction in second-generation free radicals that would be necessary to sustain the chain reactions leading to ketones. Another significant prediction was that limiting the oxygen composition in the package to below 6% during shelf aging would not only reduce the magnitude of oxidation but also shift the oxidation maximum from the subsurface to the surface, thereby eliminating the potential for white-band formation.

The predictions of all four models with respect to ketone concentration profiles were similar in many respects. This observation stresses the importance of monitoring as many species as possible to identify the appropriate model and the correct chemistry without ambiguity. Although it may be easier to measure only the ketones in UHMWPE samples, that alone is insufficient to completely identify the chemistry that occurs in such complex systems.

V. Medhekar received partial support from the Chemical Engineering Department of Worcester Polytechnic Institute (Worcester, MA). The authors acknowledge the helpful comments of J. H. Dumbleton.

APPENDIX

$$\frac{\partial[O_2]}{\partial t} = D\frac{\partial^2[O_2]}{\partial x^2} - k_1[O_2][R^*] - k_3[R'^*][O_2]$$

$$\frac{\partial[R^*]}{\partial t} = -k_1[R^*][O_2] - k_4\{[R'O_2^*][R^*] + [RO_2^*][R^*]\}$$

$$\frac{\partial[RO_2^*]}{\partial t} = k_1[R^*][O_2] - k_2[RO_2^*][RH] - k_4\{[RO_2^*][R'^*] + [RO_2^*][R^*]\} - k_5[RO_2^*][ROOH][RH]$$

$$\frac{\partial[R'^*]}{\partial t} = k_2[RH][RO_2^*] - k_3[R'^*][O_2] + k_4\{[R'^*][R'O_2^*] + [R'O_2^*][R^*] + [RO_2^*][R'^*] + [RO_2^*][R^*]\} + k_5\{[RO_2^*][ROOH][RH] + [R'O_2^*][ROOH][RH]\}$$

$$\frac{\partial[R'O_2^*]}{\partial t} = k_3[R'^*][O_2] - k_4\{[R'O_2^*][R'^*] + [R'O_2^*][R^*]\} - k_5[R'O_2^*][ROOH][RH]$$

$$\frac{\partial[RCO]}{\partial t} = 2k_4\{[R'^*][R'O_2^*] + [R'O_2^*][R^*] + [RO_2^*][R'^*] + [RO_2^*][R^*]\} + k_5\{[RO_2^*][ROOH][RH] + [R'O_2^*][ROOH][RH]\}$$

$$\frac{\partial[ROOH]}{\partial t} = k_2[RO_2^*][RH] - k_6[ROOH]$$

References

1. Agrawal, C. M. JOM 1998, 1, 31.
2. Malchau, H.; Herberts, P.; Soderman, P.; Oden, A. Presented at the 67th Annual Meeting of the American Academy of Orthopaedic Surgeons, New Orleans, LA, March 15–19, 2000.

3. Robertsson, O.; Knutson, K.; Lewold, S.; Lidgren, L. Presented at the 68th Annual Meeting of the American Academy of Orthopaedic Surgeons, San Francisco, CA, Feb 28–March 4, 2001.
4. Goldring, S. R.; Schiller, A.; Roelke, M.; Rourke, C. M.; O'Neill, D. A.; Harris, W. H. J Bone Joint Surg A 1983, 65, 575.
5. Wroblewski, B. M. J Bone Joint Surg B 1985, 67, 757.
6. Rimnac, C. M.; Wilson, P. D., Jr.; Fuchs, M. D.; Wright, T. M. Orthrop Clin North Am 1988, 19, 631.
7. Clark, I. C., Campbell, P.; Kossousky, N. ASTM STP 1144 KR; American Society for Testing and Materials: Philadelphia, 1992; p 7.
8. Jasty, M.; Goetz, D. D.; Bragdon, C. R.; Lee, K. R.; Hanson, A. E.; Elder, J. R.; Harris, W. H. J Bone Joint Surg 1997, 79, 349.
9. Premnath, V.; Harris, W. H.; Jasty, M.; Merrill, E. W. Biomaterials 1996, 17, 1741.
10. Costa, L.; Luda, M. P.; Trossarelli, L.; Brach del Prever, E. M.; Crova, M.; Gallinaro, P. Biomaterials 1998, 19, 659.
11. Costa, L.; Luda, M. P.; Trossarelli, L.; Brach del Prever, E. M.; Crova, M.; Gallinaro, P. Biomaterials 1998, 19, 1371.
12. Daly, B. M.; Yin, J. J Biomed Mater Res 1998, 42, 523.
13. Coote, C. F.; Hamilton, J. V.; McGimpsey, W. G.; Thompson, R. W. J Appl Polym Sci 2000, 77, 2525.
14. Flynn, M. M.S. Thesis, Worcester Polytechnic Institute, 1996.
15. Sun, D. C.; Schmidig, G.; Stark, C.; Dumbleton, J. H. Transactions, Proceedings of the 21st Annual Meeting of the Society for Biomaterials, Society of Biomaterials, San Francisco, CA, March 18–22, 1995, Vol 18.
16. Goldman, M.; Gronsky, R.; Long, G. G.; Pruitt, L. Polym Degrad Stab 1998, 62, 97.
17. Kennedy, F. E.; Currier, J. H.; Plumet, S.; Duda, J. L.; Gestwick, D. P.; Collier, J. P.; Currier, B. H.; Dubourg, M.-C. Presented at the STLE/ASME Tribology Conference, Orlando, FL, Oct 10–13, 1999; Paper 99-Trib-28.
18. Edidin, A. A.; Jewett, C. W.; Kalinowski, A.; Kwarteng, K.; Kurtz, S. M. Biomaterials 2000, 21, 1451.
19. Sun, D. C.; Stark, C.; Dumbleton, J. H. Polym Repr 1994, 35, 969.
20. Sun, D. C.; Schmidig, G.; Stark, C.; Dumbleton, J. H. Orthop Res Soc 1996, 42, 493.
21. Yeom, B.; Yu, Y.-J.; McKellop, H. A.; Salovey, R. J Polym Sci Part A: Polym Chem 1998, 36, 329.
22. William, J. L. In Radiation Effects on Polymers; Clough, R. L.; Shalaby, S. W.; American Chemical Society: Washington, DC, September, 1991; Chapter 35, p 554. (Published as book from proceedings of ACS Symposium Series No. 475, 200th national meeting, Washington, DC, August 1990.)
23. Costa, L.; Luda, M. P.; Trossarelli, L. Polym Degrad Stab 1997, 55, 329.
24. Costa, L.; Luda, M. P.; Trossarelli, L. Polym Degrad Stab 1997, 58, 41.
25. Petrůj, J.; Marchal, J. Radiat Phys Chem 1979, 16, 27.
26. Matsuo, H.; Dole, M. J Chem Phys 1959, 63, 837 and references therein to Bach, N. Presented at the International Radiation Research Congress, Burlington, VT, Aug 1958.
27. Pauly, S. Polymer Handbook; Brandup, J.; Immergut, E. H.; Grulke, L. A.; Akihiro, A.; Bloch, D., Eds.; John Wiley & Sons: New York, Feb 22, 1999.
28. Premnath, V.; Bellare, A.; Merrill, E. W.; Jasty, M.; Harris, W. H. Polymer 1999, 40, 2215.
29. Torikai, A.; Goetha, R.; Nagaya, S.; Fueki, K. Polym Degrad Stab 1986, 16, 199.
30. Nakamura, K.; Ogata, S.; Ikada, Y. Biomaterials 1998, 19, 2341.
31. O'Neill, P.; Birkinshaw, C.; Leahy, J. J.; Barklie, R. Polym Degrad Stab 1999, 63, 31.
32. Wang, A. Stryker Howmedica Osteonics, Inc., Worcester, MA, personal communication, Dec 2000.
33. Gugumus, F. Polym Degrad Stab 2000, 68, 337.